Ukrainian Journal of Physical Optics
ISSUE 1
2025

THERMAL EXPANSION AND VIBRATIONAL SPECTRA OF PARATELLURITE IN QUASI-HARMONIC APPROXIMATION

SYETOV Y.

Department of Experimental Physics, Oles Honchar Dnipro National University,
72, Nauky Ave., Dnipro, 49010, Ukraine. e-mail: setov2003@yahoo.com

Received: 02.12.2024

Abstract. Thermal expansion of the paratellurite is modeled with density functional theory calculations using quasi-harmonic approximation. The calculations qualitatively reproduce anisotropy of the thermal expansion and demonstrate good correspondence to the experimental values at low temperatures. Lattice vibrations at the Γ-point are described in terms of the motion of the TeO_2 fragments, and the temperature shift of frequencies in vibrational spectra is evaluated.

Keywords: paratellurite, thermal expansion, phonons, vibrational spectra
UDC: 539.8: 538.958
DOI: 10.3116/16091833/Ukr.J.Phys.Opt.2025.01XXX

1. Introduction

Paratellurite α-TeO_2 is a widely used material in acousto-optics for decades [1]; recent studies probe paratellurite as an ultrawide bandgap semiconductor for thin-film transistor (TFT) devices [2] and nanostructures [3,4]. Paratellurite demonstrates anisotropic linear thermal expansion with different coefficients for directions parallel and perpendicular to the symmetry axis of the highest order. Thermal expansion coefficients depend on temperature [1, 5-7]. The anisotropic expansion leads to the deformation of surfaces of elements of optoelectronic devices with increasing temperature. This surface distortion complicates the thermo-compression welding process, which is used for the fabrication of acousto-optic devices when the piezoelectric transducer and the TeO_2 crystal are heated to about 200° C [1].

Microscopic calculations of structure, electronic, vibrational spectra, and properties of paratellurite were performed with the density functional theory (DFT) methods [8-12]. The results of these studies demonstrate good correspondence to experimental data. Theoretical modeling considered the influence of pressure on the elastic, electronic, and optical properties [8], the dependence of structure on volume variation [12], and thermal volume expansion [10]. Calculations of the thermal expansion of crystals by minimization of the Helmholtz free energy in relation to the lattice parameters allow us to evaluate the thermal expansion components in different directions [13].

In the present work we model thermal expansion effects in paratellurite with calculation of changes in the Helmholtz free energy with variation of lattice parameters for the first time.

2. Calculations details

All computations were carried out using DFT with the projector augmented plane-wave method and PBEsol functional [14] as implemented in the Quantum ESPRESSO program

[15,16]. It was found that using the PBEsol functional provides better correspondence to the experimental value of a specific volume of paratellurite crystal [9]. The plane-wave energy cutoff is 50 Ry, and the k-point grid is 3×3×2. The structure optimization was performed with the final forces below 10^{-5} Ry/Bohr. The phonon calculations were performed using a 2×2×2 q-point grid.

Temperature-dependent lattice parameters were found by minimization of Helmholtz free energy. The Helmholtz energy of a crystal solid in the quasi-harmonic approximation is

$$F(T,X)=U_0(T,X)+F^{vib}(T,X)+F^{el}(T,X), \tag{1}$$

where U_0 is the static energy at 0 K, F^{vib} is the contribution due to lattice vibrations, and F^{el} is the energy due to electronic excitations.

In the adiabatic approximation, each term is considered separately, F^{el} is not taken into account in the present calculations. X are variable parameters, in case of tetragonal cell they are the two lattice parameters a and c/a. For a given X, the vibrational Helmholtz energy per cell is calculated as in the harmonic approximation:

$$F^{vib}(T,X)=\frac{1}{2N}\sum_{\vec{q},\nu}\hbar\omega(\vec{q},\nu,X)+\frac{k_BT}{N}\sum_{\vec{q},\nu}\ln\left[1-\exp\left(\frac{-\hbar\omega(\vec{q},\nu,X)}{k_BT}\right)\right]. \tag{2}$$

where ν is the different phonon branches, $\vec{q}$ is the wavevectors of phonons, k_B is the Boltzmann constant, $\hbar$ is the reduced Planck constant, T is the absolute temperature, and N is the number of unit cells in the solid.

The first term on the right-hand side of equation (2) is the zero-point energy, and the second is the phonon contribution at finite temperatures. The sums are taken over the phonon frequencies $\omega(\vec{q},\nu,X)$ and the wavevectors within the first Brillouin zone. The calculations are carried out on a grid of points of a and c/a. Then, the Helmholtz energy at each T was fitted with the quartic polynomial surface as a function of a and c/a with the subsequent search for a minimum [13].

The Helmholtz free energy was calculated for the grid with variation of lattice parameters by -0.1 +0.15 Å by step 0.05 Å for a and ±0.04 by step 0.02 for the relation c/a around the optimized structure, keeping the symmetry of the unit cell. Free energy was calculated with the Thermo_pw program [17]. At fixed lattice parameters that correspond to the minimum of the fitted free energy, the positions of the atoms in the cell are optimized to minimize energy and frequencies of phonons at the Γ-point were calculated with the harmonic approximation (quasi-harmonic model).

3. Results and discussion

The crystal structure of paratellurite has tetragonal symmetry ($P4_12_12$) with four formula units in the unit cell (Fig. 1a). A Te atom in the lattice is surrounded by four oxygen atoms (Fig. 1b); the distances Te-O are different for two pairs of oxygen atoms. Lattice parameters obtained by our calculations are close to the ones reported in [9]. The calculated lattice parameters, Te-O distances and O-Te-O angles are within the accuracy of the DFT methods used earlier for the structure modeling of paratellurite crystal (Table 1). The total energy per unit cell is obtained to be -1756.12945128 Ry. The angles O1-Te-O2' and O1-Te-O2 are calculated to be 88.1° and 83.6°. Compared with the X-ray diffraction data [18], the calculations overestimate lattice parameter a and underestimate the parameter c.

Interatomic distances Te-O are overestimated by the calculations, whereas the angles O1-Te-O1' and O2-Te-O2' are less than determined experimentally.

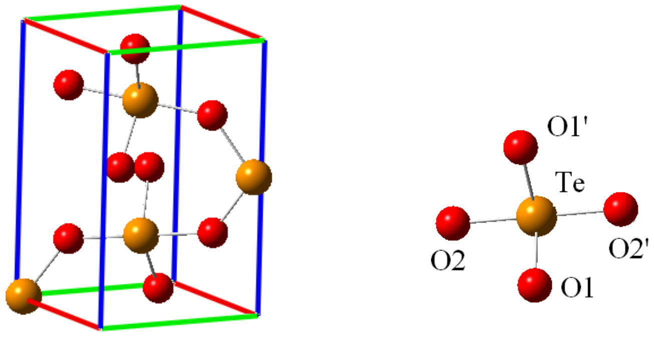

(a) (b)

Fig. 1. The unit cell of paratellurite crystal (a) and its fragment, constituted by the tellurium and nearest oxygen atoms (b).

Table 1. Structure parameters of paratellurite crystal.

	a, *b*, Å	*c*, Å	Te–O1, Å	Te–O2, Å	O1-Te-O1', deg	O2-Te-O2', deg
This work	4.838	7.414	1.937	2.141	101.7	166.8
PBEsol [9]	4.840	7.434	-	-	-	-
PBE [12]	4.990	7.546	1.944	2.118	103.6	171.2
PBE [10]	4.987	7.636	1.912	2.164		
LDA [12]	4.819	7.338	2.028	2.170	99.8	161.5
PW91 [11]	4.802	7.772	1.819	2.053		
Exp. [18]	4.808	7.612	1.878	2.122	103.4	168.0

Phonons in paratelurite at the Γ-point are classified as $4A_1 + 5A_2 + 5B_1 + 4B_2 + 9E$, modes A_2 and E are polar vibrations, modes A_1, B_1, B_2, and E are active in Raman scattering. The frequency of phonons at the Γ-point calculated in harmonic approximation demonstrates a deviation from the observed in the reported spectra [19-21] less than that is obtained with the PBE functional in work [12] (Table 2). The phonon dispersion, including a contribution of the long-ranged electric field, is shown in Fig. 2a. For the Γ-point, the maximum deviation of frequencies from experimental values is about -19%. In the region above 500 cm^{-1}, the frequencies are underestimated by the calculations by less than 15%. Low frequencies up to 131 cm^{-1} are overestimated; in this region, the largest deviation is demonstrated by the vibration with A_2 symmetry 97 cm^{-1}, where the difference is about +15%. The difference in the interaction between the Te atom and two pairs of the O atoms leads to the model interpretation of the lattice as coupled TeO_2 fragments (“molecules”), considering the vibrations as changing internal coordinates, translations, and librations [19].

Internal coordinates for vibrations of a three-atom non-linear molecule similar to the TeO_2 structure can be chosen as the Te-O distances r_{31}, r_{32} and O-Te-O angle ϕ; displacements of the atoms in the internal coordinates (S_1, S_2, S_3) are related to Cartesian displacements $\vec{\rho}_1, \vec{\rho}_2, \vec{\rho}_3$ as [22]

$$S_t = \sum_{i=1}^{3} \vec{s}_{ti}\vec{\rho}_i, \quad \vec{s}_{11} = \vec{e}_{31}, \vec{s}_{13} = -\vec{e}_{31}, \vec{s}_{12} = 0, \vec{s}_{21} = 0, \vec{s}_{23} = -\vec{e}_{32}, \vec{s}_{22} = \vec{e}_{32},$$

$$S_3 = \Delta\phi = \left(\frac{\cos\phi\vec{e}_{31} - \vec{e}_{32}}{r_{31}\sin\phi}\right)\vec{\rho}_1 + \left(\frac{\cos\phi\vec{e}_{32} - \vec{e}_{31}}{r_{32}\sin\phi}\right)\vec{\rho}_2 + \left(\frac{(r_{31} - r_{32}\cos\phi)\vec{e}_{\mathbf{31}} + (r_{32} - r_{31}\cos\phi)\vec{e}_{\mathbf{32}}}{r_{31}r_{32}\sin\phi}\right)\vec{\rho}_3, \quad (3)$$

where $\vec{e}_{31}$ and $\vec{e}_{32}$ are unit vectors along the Te-O directions. The value $(r_{31}r_{32})^{1/2}\Delta\phi$ is considered when comparing changes in the angle to stretching coordinates.

Table 2. Phonon frequencies of α-TeO_2 at the Γ-point. The contribution of the long-ranged electric field is not included (LO-TO splitting). Experimental values for the vibrations with the symmetry E are shown for TO phonons

Symmetry	Calculated, cm^{-1}						Experimental, cm^{-1}				
	Harmonic approximation		Quasi-harmonic approximation				Raman hyper-Raman [19]	Raman 85 K [20]	IR 85 K [21]	Raman 295 K [20]	IR 295 K [21]
	This work	PBE [12]	Temperature, K: 1	85	295	502					
B_1	65	62	66	66	66	66	62	62	-	62	-
A_2	97	90	96	96	95	94	82	-	-	-	82
E	128	116	129	129	128	127	122	123	124	122	121
B_1	131	125	131	131	131	130	125	-	-	-	-
B_2	139	136	138	138	138	138	150	157	-	155	-
A_1	140	134	139	139	138	138	148	152	-	148	-
B_1	167	150	165	165	165	164	177	179	-	175	-
E	173	162	173	173	172	171	173	177	177	174	174
E	207	193	203	203	202	200	207	215	210	-	212
A_1	214	195	211	210	209	208	233	-	-	-	-
B_1	222	218	219	219	217	216	210	-	-	-	-
B_2	257	235	255	255	253	252	287	-	-	-	-
A_2	266	254	262	262	261	259	262	-	-	-	259
E	277	262	276	276	275	274	296	299	299	297	297
A_2	293	286	293	294	294	294	321	-	-	-	315
E	315	295	313	313	311	309	336	-	335.5	-	330
E	325	317	323	323	322	320	392	-	379.4	-	379.4
A_1	377	364	374	373	372	370	393	392	-	393	-
B_2	398	385	395	395	394	392	415	415	-	414	-
A_2	519	515	517	517	518	518	592	-	-	575	-
B_1	522	509	519	519	519	519	590	589	-	591	-
E	587	567	586	586	586	585	646	642	644	-	643
A_1	591	575	588	588	588	588	648	649	-	648	-
E	701	694	699	699	699	699	767	769	774	767	769
B_2	713	706	711	711	711	711	784	786	-	784	-

Molecular normal modes should satisfy the Eckart conditions [22]

$$\sum_{i=1}^{3} m_i \vec{\rho}_i = 0, \quad (4)$$

$$\sum_{i=1}^{3} m_i \left[\vec{r}_i^{\,0}, \vec{\rho}_i \right] = 0, \quad (5)$$

where m_i and $\vec{r}_i^{\,0}$ are mass and the equilibrium position radius-vector of atom *i*.

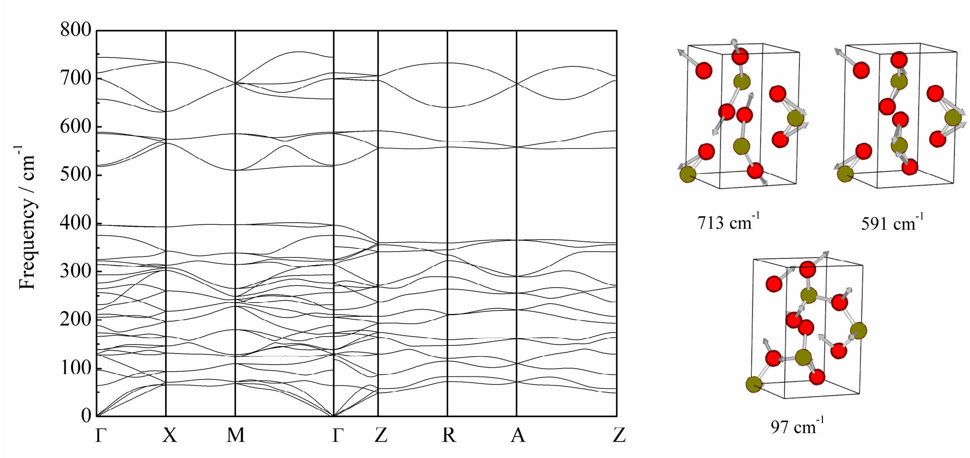

(a) (b)

Fig. 2. Phonon dispersion in paratellurite, calculated with the harmonic approximation (a) and displacements of atoms during some lattice vibrations at the Γ-point (b).

Calculation of changes of internal coordinates, displacements of the centers of mass, and the left parts of the rotational Eckart conditions (5) in the principal axis of inertia for the corresponding fragments allows us to determine mostly internal vibrations in the region above 350 cm^{-1}: bending vibrations with calculated frequencies 377, 398 cm^{-1} and stretching with frequencies 713, 701, 591, 587, 522, 519 cm^{-1}. In contrast to vibrations in the isolated molecule, the symmetric stretching vibrations of the fragments in the crystal 591 and 713 cm^{-1} demonstrate larger frequencies than anti-symmetric 519 and 522 cm^{-1}. The contribution of changes in O1-Te-O1' angles to the symmetric stretching vibrations is larger than in molecular vibrations (Fig. 2b). It shows that the interaction of the TeO_2 fragment with the remaining oxygen atoms is strong. The bending of the TeO_2 fragment is noticeably involved in the vibrations 325, 315, 277, 213, 173, 140, and 139 cm^{-1}, where it is mixed with mostly librations (325-215 cm^{-1}) and mostly translations (139 cm^{-1}). The vibrations 173, 140 cm^{-1} include both translations and librations. Mostly librational are the vibrations 293, 266, 257, 221, 130 cm^{-1}; mostly translational are 167, 207 cm^{-1}, remaining vibrations can be considered as mixed translations and librations of the fragment. Such separation of the motion of the fragment to internal, translational, and librational vibrations is approximate.

The dependence of the lattice parameters on temperature predicted by the quasi-harmonic model is shown in Fig. 3a. Components of the thermal expansion coefficient tensor are obtained by numerical differentiation of the dependence of cell parameters on temperature. The results qualitatively reproduce the anisotropy of the thermal expansion. The calculated expansion coefficients correspond well to the reported experimental values at temperatures below 200 K (Fig. 3b). In the region above 200 K, the calculated values agree well with the data reported in [6] for the expansion parallel to the axis *c*. In contrast, for the expansion perpendicular to the axis c, the modeling underestimates the value. The larger deviation at higher temperatures may be attributed to approximations of the model that does not exactly describe the anharmonicity of vibrations and treats phonons as independent.

Upon increasing volume, the distances Te-O2 increases, while Te-O1 decreases (Fig. 4a). The angles O1-Te-O1', O1-Te-O2, O1-Te-O2', O2-Te-O2' increases; the most pronounced is change in the value of the angle O2-Te-O2' (Fig. 4b). The change of angles and distances is in correspondence with the results reported in [12] for variation of cell volume and supports the separation of TeO_2 fragments. The structure and vibrations of an isolated TeO_2 molecule were estimated by calculation on the lattice with parameter 15 Å using a cubic unit cell containing one molecule. The calculations yield the Te-O bond length 1.819 Å, O-Te-O angle 110.8°; frequencies 179 cm^{-1} for bending, 823 cm^{-1} for symmetric stretching, and 860 cm^{-1} for anti-symmetric stretching modes.

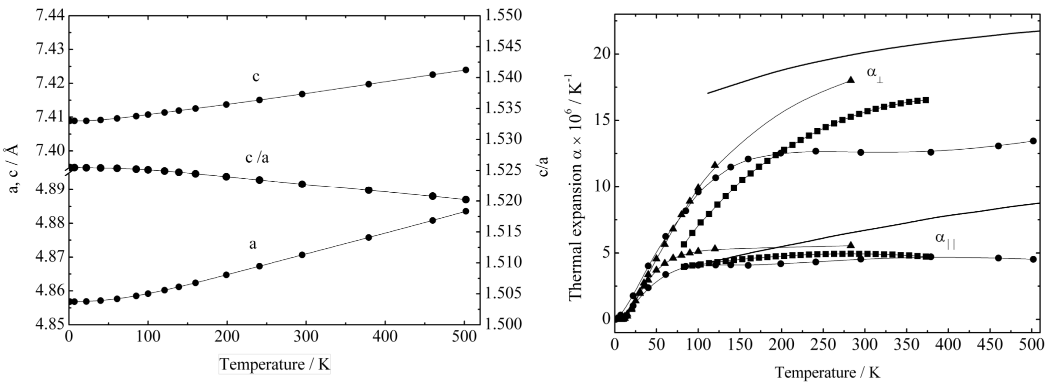

(a) (b)

Fig. 3. Temperature dependencies of the (a) lattice parameters (*a*, *c*, *c*/*a*), (b) thermal expansion coefficients parallel $\alpha_{\parallel}$ and perpendicular $\alpha_{\perp}$ to the c-axis: calculated (circles), experimental ([5] – triangles, [6] – squares, [7] – solid line).

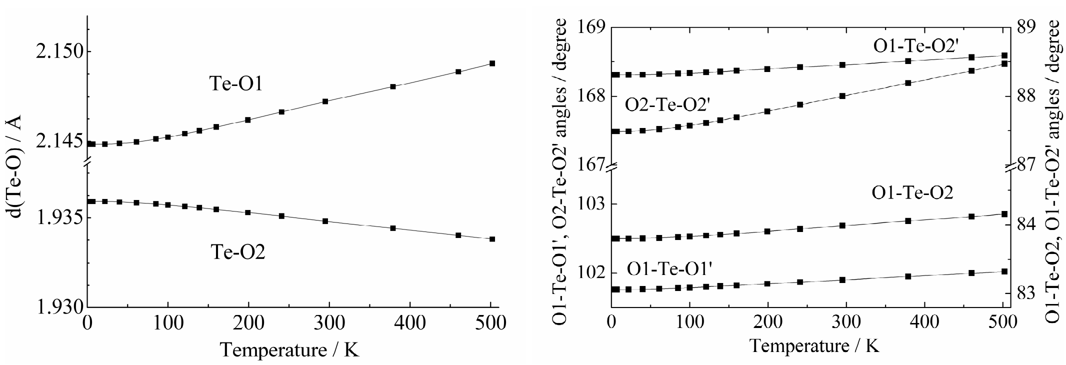

(a) (b)

Fig. 4. Calculated bond lengths (a) and bond angles (b) of the crystal lattice of α-TeO_2 as a function of temperature.

Calculations of vibrational frequencies ω for phonons at the Γ-point for the expanding cell volume corresponding to different temperatures predict decreasing frequency for most vibrations except the vibrations 65, 293 cm^{-1} and stretching vibration 713 cm^{-1}; this positive shift is less than 0.5 cm^{-1} in the temperature range 1-500 K (Table 2). The negative shift is calculated not to exceed 4 cm^{-1}, and the largest shift is found for the vibrations in the region 200-400 cm^{-1} except for the vibration 293 cm^{-1}. The largest relative shift $\Delta\omega/\omega$ is found for the vibration with a calculated frequency 97 cm^{-1} (Fig. 2b), which can be considered as the motion of the TeO_2 fragment involving translations along the directions *a* and *b* and libration around the principal axis of inertia perpendicular to the plane of the fragment.

Comparison with the available experimental data on the vibration frequencies derived from IR and Raman spectra [20,21] demonstrates that the quasi-harmonic approximation underestimates the temperature shift (Table 2). The calculated maximum shift between the frequencies at 85 K and 295 K is about 2 cm^{-1}, while the maximum experimental shift is 5 cm^{-1} (Table 1). The quasi-harmonic approximation provides only part of the frequency shift because it does not include anharmonicity of the vibrations [23].

4. Conclusions

The thermal expansion of paratellurite is studied by microscopic calculations with density functional theory methods in quasi-harmonic approximation. Values of components of the thermal expansion coefficient tensor are obtained at different temperatures. The calculated thermal expansion coefficients agree well with experimental data at temperature below 200 K, at higher temperatures the calculations reproduce anisotropy of thermal expansion but underestimate the numerical values. It was found that the changes in volume are caused by the increase in the distance between TeO_2 fragments (elongation of the bonds between the Te atom and more distant coordinated O atoms, as well as an increase in the angle between these bonds). Lattice vibrations at the Γ-point are analyzed in terms of internal and external vibrations of the TeO_2 fragments. It was shown that there is a region of frequencies where the internal bending of the fragments is mixed with external motions. The temperature shift of the frequencies of phonons at the Γ-point predicted by the model is lower than observed in experiments.

Disclosures. The authors declare no conflicts of interest

References

1. Goutzoulis, A. P. (2021). *Design and fabrication of acousto-optic devices*. CRC Press.
2. Devabharathi, N., Yadav, S., Dönges, I., Trouillet, V., & Schneider, J. J. (2024). α-TeO_2 oxide as transparent p-type semiconductor for low temperature processed thin film transistor devices. *Advanced Materials Interfaces*, *11*(16), 2301082.
3. Mayer, R. A., Wehmeier, L., Torquato, M., et al. (2024). Paratellurite nanowires as a versatile material for THz phonon polaritons. *ACS Photonics*, *11*(10), 4323-4333.
4. Subedi, R., & Guisbiers, G. (2024). Synthesis of ultrawide band gap TeO_2 nanoparticles by pulsed laser ablation in liquids: Top ablation versus bottom ablation. *ACS Omega*.
5. White, G. K., Collocott, S. J., & Collins, J. G. (1990). Thermal properties of paratellurite (TeO_2) at low temperatures. *Journal of Physics: Condensed Matter*, *2*(37), 7715.
6. Silvestrova, I. M., Pisarevskii, Y. V., Senyushenkov, P. A., Krupny, A. I., Voszka, R., Földvári, I., & Janszky, J. (1987). Temperature dependence of elastic properties of paratellurite. *Phys. Status Solidi A;(German Democratic Republic)*, *101*(2).
7. Ohmachi, Y., & Uchida, N. (1970). Temperature dependence of elastic, dielectric, and piezoelectric constants in TeO_2 single crystals. *Journal of Applied Physics*, *41*(6), 2307-2311.
8. Gao, S., Zhang, X., Zeng, Q., & Wang, S. (2019). First-principles study of elastic, electronic, and optical properties of α-TeO_2 under pressure. *Journal of Alloys and Compounds*, *776*, 417-427.
9. Roginskii, E. M., Smirnov, M. B., Kuznetsov, V. G., Noguera, O., Cornette, J., Masson, O., & Thomas, P. (2019). A computational study of the electronic structure and optical properties of the complex TeO_2/TeO_3 oxides as advanced materials for nonlinear optics. *Materials Research Express*, *6*(12), 125903.

10. Deringer, V. L., Stoffel, R. P., & Dronskowski, R. (2014). Thermochemical ranking and dynamic stability of TeO_2 polymorphs from ab initio theory. *Crystal Growth & Design*, *14*(2), 871-878.
11. Li, Y., Fan, W., Sun, H., Cheng, X., Li, P., & Zhao, X. (2010). Structural, electronic, and optical properties of α, β, and γ-TeO_2. *Journal of Applied Physics*, *107*(9).
12. Ceriotti, M., Pietrucci, F., & Bernasconi, M. (2006). Ab initio study of the vibrational properties of crystalline TeO_2: The α, β, and γ phases. *Physical Review B—Condensed Matter and Materials Physics*, *73*(10), 104304.
13. Palumbo, M., & Dal Corso, A. (2017). Lattice dynamics and thermophysical properties of hcp Os and Ru from the quasi-harmonic approximation. *Journal of Physics: Condensed Matter*, *29*(39), 395401.
14. Perdew, J. P., Ruzsinszky, A., Csonka, G. I., Vydrov, O. A., Scuseria, G. E., Constantin, L. A., Zhou, X. & Burke, K. (2008). Restoring the density-gradient expansion for exchange in solids and surfaces. *Physical Review Letters*, *100*(13), 136406.
15. Giannozzi, P., Baroni, S., Bonini, et al. (2009). QUANTUM ESPRESSO: a modular and open-source software project for quantum simulations of materials. *Journal of Physics: Condensed Matter*, *21*(39), 395502.
16. Giannozzi, P., Andreussi, O., Brumme, et al. (2017). Advanced capabilities for materials modelling with Quantum ESPRESSO. *Journal of Physics: Condensed Matter*, *29*(46), 465901.
17. https://dalcorso.github.io/thermo_pw/
18. Thomas, P. A. (1988). The crystal structure and absolute optical chirality of paratellurite, α-TeO_2. *Journal of Physics C: Solid State Physics*, *21*(25), 4611.
19. Rodriguez, V., Couzi, M., Adamietz, F., Dussauze, M., Guery, G., Cardinal, T., Veber, P., Richardson, K. & Thomas, P. (2013). Hyper-Raman and Raman scattering in paratellurite TeO_2. *Journal of Raman Spectroscopy*, *44*(5), 739-745.
20. Pine, A. S., & Dresselhaus, G. (1972). Raman scattering in paratellurite, TeO_2. *Physical Review B*, *5*(10), 4087.
21. Korn, D. M., Pine, A. S., Dresselhaus, G., & Reed, T. B. (1973). Infrared reflectivity of paratellurite, TeO_2. *Physical Review B*, *8*(2), 768.
22. Wilson, E. B., Decius, J. C., & Cross, P. C. (1980). *Molecular vibrations: the theory of infrared and Raman vibrational spectra*. Courier Corporation.
23. Allen, P. B. (2020). Theory of thermal expansion: Quasi-harmonic approximation and corrections from quasi-particle renormalization. *Modern Physics Letters B*, *34*(02), 2050025.

Syetov Y. (2025). Thermal Expansion and Vibrational Spectra of Paratellurite in Quasi-Harmonic Approximation**.** *Ukrainian Journal of Physical Optics*, *26*(1), 01032 – 01039.
doi: 10.3116/16091833/Ukr.J.Phys.Opt.2025.01032

Анотація. *Теплове розширення парателуриту моделюється за допомогою розрахунків теорії функціоналу густини з використанням квазігармонійного наближення. Розрахунки якісно відтворюють анізотропію теплового розширення та демонструють добру відповідність експериментальним значенням при низьких температурах. Коливання ґратки в Γ-точці описано в рамках руху фрагментів TeO_2 та оцінено температурний зсув частот у коливальних спектрах.*

Ключові слова: *парателурит, теплове розширення, фонони, коливальні спектри.*